

Search for rare quark-annihilation decays, $B^- \rightarrow D_s^{(*)-} \phi$

B. Aubert,¹ R. Barate,¹ D. Boutigny,¹ F. Couderc,¹ Y. Karyotakis,¹ J. P. Lees,¹ V. Poireau,¹ V. Tisserand,¹
A. Zghiche,¹ E. Grauges,² A. Palano,³ M. Pappagallo,³ A. Pompili,³ J. C. Chen,⁴ N. D. Qi,⁴ G. Rong,⁴
P. Wang,⁴ Y. S. Zhu,⁴ G. Eigen,⁵ I. Ofte,⁵ B. Stugu,⁵ G. S. Abrams,⁶ M. Battaglia,⁶ D. Best,⁶ A. B. Breon,⁶
D. N. Brown,⁶ J. Button-Shafer,⁶ R. N. Cahn,⁶ E. Charles,⁶ C. T. Day,⁶ M. S. Gill,⁶ A. V. Gritsan,⁶ Y. Groysman,⁶
R. G. Jacobsen,⁶ R. W. Kadel,⁶ J. Kadyk,⁶ L. T. Kerth,⁶ Yu. G. Kolomensky,⁶ G. Kukartsev,⁶ G. Lynch,⁶
L. M. Mir,⁶ P. J. Oddone,⁶ T. J. Orimoto,⁶ M. Pripstein,⁶ N. A. Roe,⁶ M. T. Ronan,⁶ W. A. Wenzel,⁶ M. Barrett,⁷
K. E. Ford,⁷ T. J. Harrison,⁷ A. J. Hart,⁷ C. M. Hawkes,⁷ S. E. Morgan,⁷ A. T. Watson,⁷ M. Fritsch,⁸ K. Goetzen,⁸
T. Held,⁸ H. Koch,⁸ B. Lewandowski,⁸ M. Pelizaeus,⁸ K. Peters,⁸ T. Schroeder,⁸ M. Steinke,⁸ J. T. Boyd,⁹
J. P. Burke,⁹ W. N. Cottingham,⁹ T. Cuhadar-Donszelmann,¹⁰ B. G. Fulsom,¹⁰ C. Hearty,¹⁰ N. S. Knecht,¹⁰
T. S. Mattison,¹⁰ J. A. McKenna,¹⁰ A. Khan,¹¹ P. Kyberd,¹¹ M. Saleem,¹¹ L. Teodorescu,¹¹ A. E. Blinov,¹²
V. E. Blinov,¹² A. D. Bukin,¹² V. P. Druzhinin,¹² V. B. Golubev,¹² E. A. Kravchenko,¹² A. P. Onuchin,¹²
S. I. Serebnyakov,¹² Yu. I. Skovpen,¹² E. P. Solodov,¹² A. N. Yushkov,¹² M. Bondioli,¹³ M. Bruinsma,¹³ M. Chao,¹³
S. Curry,¹³ I. Eschrich,¹³ D. Kirkby,¹³ A. J. Lankford,¹³ P. Lund,¹³ M. Mandelkern,¹³ R. K. Mommsen,¹³
W. Roethel,¹³ D. P. Stoker,¹³ C. Buchanan,¹⁴ B. L. Hartfiel,¹⁴ S. D. Foulkes,¹⁵ J. W. Gary,¹⁵ O. Long,¹⁵
B. C. Shen,¹⁵ K. Wang,¹⁵ L. Zhang,¹⁵ D. del Re,¹⁶ H. K. Hadavand,¹⁶ E. J. Hill,¹⁶ D. B. MacFarlane,¹⁶
H. P. Paar,¹⁶ S. Rahatlou,¹⁶ V. Sharma,¹⁶ J. W. Berryhill,¹⁷ C. Campagnari,¹⁷ A. Cunha,¹⁷ B. Dahmes,¹⁷
T. M. Hong,¹⁷ M. A. Mazur,¹⁷ J. D. Richman,¹⁷ W. Verkerke,¹⁷ T. W. Beck,¹⁸ A. M. Eisner,¹⁸ C. J. Flacco,¹⁸
C. A. Heusch,¹⁸ J. Kroseberg,¹⁸ W. S. Lockman,¹⁸ G. Nesom,¹⁸ T. Schalk,¹⁸ B. A. Schumm,¹⁸ A. Seiden,¹⁸
P. Spradlin,¹⁸ D. C. Williams,¹⁸ M. G. Wilson,¹⁸ J. Albert,¹⁹ E. Chen,¹⁹ G. P. Dubois-Felsmann,¹⁹ A. Dvoretzskii,¹⁹
D. G. Hitlin,¹⁹ J. S. Minamora,¹⁹ I. Narsky,¹⁹ T. Piatenko,¹⁹ F. C. Porter,¹⁹ A. Ryd,¹⁹ A. Samuel,¹⁹
R. Andreassen,²⁰ G. Mancinelli,²⁰ B. T. Meadows,²⁰ M. D. Sokoloff,²⁰ F. Blanc,²¹ P. C. Bloom,²¹ S. Chen,²¹
W. T. Ford,²¹ J. F. Hirschauer,²¹ A. Kreisel,²¹ U. Nauenberg,²¹ A. Olivas,²¹ W. O. Ruddick,²¹ J. G. Smith,²¹
K. A. Ulmer,²¹ S. R. Wagner,²¹ J. Zhang,²¹ A. Chen,²² E. A. Eckhart,²² A. Soffer,²² W. H. Toki,²² R. J. Wilson,²²
F. Winklmeier,²² Q. Zeng,²² D. Altenburg,²³ E. Feltresi,²³ A. Hauke,²³ B. Spaan,²³ T. Brandt,²⁴ J. Brose,²⁴
M. Dickopp,²⁴ V. Klose,²⁴ H. M. Lacker,²⁴ R. Nogowski,²⁴ S. Otto,²⁴ A. Petzold,²⁴ J. Schubert,²⁴ K. R. Schubert,²⁴
R. Schwierz,²⁴ J. E. Sundermann,²⁴ D. Bernard,²⁵ G. R. Bonneaud,²⁵ P. Grenier,²⁵ E. Latour,²⁵ S. Schrenk,²⁵
Ch. Thiebaux,²⁵ G. Vasileiadis,²⁵ M. Verderi,²⁵ D. J. Bard,²⁶ P. J. Clark,²⁶ W. Gradl,²⁶ F. Muheim,²⁶ S. Playfer,²⁶
Y. Xie,²⁶ M. Andreotti,²⁷ D. Bettoni,²⁷ C. Bozzi,²⁷ R. Calabrese,²⁷ G. Cibinetto,²⁷ E. Luppi,²⁷ M. Negrini,²⁷
L. Piemontese,²⁷ F. Anulli,²⁸ R. Baldini-Ferrolì,²⁸ A. Calcaterra,²⁸ R. de Sangro,²⁸ G. Finocchiaro,²⁸ P. Patteri,²⁸
I. M. Peruzzi,^{28,*} M. Piccolo,²⁸ A. Zallo,²⁸ A. Buzzo,²⁹ R. Capra,²⁹ R. Contri,²⁹ M. Lo Vetere,²⁹ M. M. Macri,²⁹
M. R. Monge,²⁹ S. Passaggio,²⁹ C. Patrignani,²⁹ E. Robutti,²⁹ A. Santroni,²⁹ S. Tosi,²⁹ G. Brandenburg,³⁰
K. S. Chaisanguanthum,³⁰ M. Morii,³⁰ J. Wu,³⁰ R. S. Dubitzky,³¹ U. Langenegger,³¹ J. Marks,³¹ S. Schenk,³¹
U. Uwer,³¹ W. Bhimji,³² D. A. Bowerman,³² P. D. Dauncey,³² U. Egede,³² R. L. Flack,³² J. R. Gaillard,³² J.
.A. Nash,³² M. B. Nikolich,³² W. Panduro Vazquez,³² X. Chai,³³ M. J. Charles,³³ W. F. Mader,³³ U. Mallik,³³
V. Ziegler,³³ J. Cochran,³⁴ H. B. Crawley,³⁴ L. Dong,³⁴ V. Eyges,³⁴ W. T. Meyer,³⁴ S. Prell,³⁴ E. I. Rosenberg,³⁴
A. E. Rubin,³⁴ J. I. Yi,³⁴ G. Schott,³⁵ N. Arnaud,³⁶ M. Davier,³⁶ X. Giroux,³⁶ G. Grosdidier,³⁶ A. Höcker,³⁶ F. Le
Diberder,³⁶ V. Lepeltier,³⁶ A. M. Lutz,³⁶ A. Oyanguren,³⁶ T. C. Petersen,³⁶ S. Plaszczynski,³⁶ S. Rodier,³⁶
P. Roudeau,³⁶ M. H. Schune,³⁶ A. Stocchi,³⁶ W. F. Wang,³⁶ G. Wormser,³⁶ C. H. Cheng,³⁷ D. J. Lange,³⁷
D. M. Wright,³⁷ A. J. Bevan,³⁸ C. A. Chavez,³⁸ I. J. Forster,³⁸ J. R. Fry,³⁸ E. Gabathuler,³⁸ R. Gamet,³⁸
K. A. George,³⁸ D. E. Hutchcroft,³⁸ R. J. Parry,³⁸ D. J. Payne,³⁸ K. C. Schofield,³⁸ C. Touramanis,³⁸
F. Di Lodovico,³⁹ W. Menges,³⁹ R. Sacco,³⁹ C. L. Brown,⁴⁰ G. Cowan,⁴⁰ H. U. Flaecher,⁴⁰ M. G. Green,⁴⁰
D. A. Hopkins,⁴⁰ P. S. Jackson,⁴⁰ T. R. McMahon,⁴⁰ S. Ricciardi,⁴⁰ F. Salvatore,⁴⁰ D. N. Brown,⁴¹ C. L. Davis,⁴¹
J. Allison,⁴² N. R. Barlow,⁴² R. J. Barlow,⁴² Y. M. Chia,⁴² C. L. Edgar,⁴² M. C. Hodgkinson,⁴² M. P. Kelly,⁴²
G. D. Lafferty,⁴² M. T. Naisbit,⁴² J. C. Williams,⁴² C. Chen,⁴³ W. D. Hulsbergen,⁴³ A. Jawahery,⁴³ D. Kovalskyi,⁴³
C. K. Lae,⁴³ D. A. Roberts,⁴³ G. Simi,⁴³ G. Blaylock,⁴⁴ C. Dallapiccola,⁴⁴ S. S. Hertzbach,⁴⁴ R. Kofler,⁴⁴
X. Li,⁴⁴ T. B. Moore,⁴⁴ S. Saremi,⁴⁴ H. Staengle,⁴⁴ S. Y. Willocq,⁴⁴ R. Cowan,⁴⁵ K. Koeneke,⁴⁵ G. Sciolla,⁴⁵

S. J. Sekula,⁴⁵ M. Spitznagel,⁴⁵ F. Taylor,⁴⁵ R. K. Yamamoto,⁴⁵ H. Kim,⁴⁶ P. M. Patel,⁴⁶ S. H. Robertson,⁴⁶ A. Lazzaro,⁴⁷ V. Lombardo,⁴⁷ F. Palombo,⁴⁷ J. M. Bauer,⁴⁸ L. Cremaldi,⁴⁸ V. Eschenburg,⁴⁸ R. Godang,⁴⁸ R. Kroeger,⁴⁸ J. Reidy,⁴⁸ D. A. Sanders,⁴⁸ D. J. Summers,⁴⁸ H. W. Zhao,⁴⁸ S. Brunet,⁴⁹ D. Côté,⁴⁹ P. Taras,⁴⁹ F. B. Viaud,⁴⁹ H. Nicholson,⁵⁰ N. Cavallo,^{51,†} G. De Nardo,⁵¹ F. Fabozzi,^{51,†} C. Gatto,⁵¹ L. Lista,⁵¹ D. Monorchio,⁵¹ P. Paolucci,⁵¹ D. Piccolo,⁵¹ C. Sciacca,⁵¹ M. Baak,⁵² H. Bulten,⁵² G. Raven,⁵² H. L. Snoek,⁵² L. Wilden,⁵² C. P. Jessop,⁵³ J. M. LoSecco,⁵³ T. Allmendinger,⁵⁴ G. Benelli,⁵⁴ K. K. Gan,⁵⁴ K. Honscheid,⁵⁴ D. Hufnagel,⁵⁴ P. D. Jackson,⁵⁴ H. Kagan,⁵⁴ R. Kass,⁵⁴ T. Pulliam,⁵⁴ A. M. Rahimi,⁵⁴ R. Ter-Antonyan,⁵⁴ Q. K. Wong,⁵⁴ N. L. Blount,⁵⁵ J. Brau,⁵⁵ R. Frey,⁵⁵ O. Igonkina,⁵⁵ M. Lu,⁵⁵ C. T. Potter,⁵⁵ R. Rahmat,⁵⁵ N. B. Sinev,⁵⁵ D. Strom,⁵⁵ J. Strube,⁵⁵ E. Torrence,⁵⁵ F. Galeazzi,⁵⁶ M. Margoni,⁵⁶ M. Morandin,⁵⁶ M. Posocco,⁵⁶ M. Rotondo,⁵⁶ F. Simonetto,⁵⁶ R. Stroili,⁵⁶ C. Voci,⁵⁶ M. Benayoun,⁵⁷ J. Chauveau,⁵⁷ P. David,⁵⁷ L. Del Buono,⁵⁷ Ch. de la Vaissière,⁵⁷ O. Hamon,⁵⁷ M. J. J. John,⁵⁷ Ph. Leruste,⁵⁷ J. Malclès,⁵⁷ J. Ocariz,⁵⁷ L. Roos,⁵⁷ G. Therin,⁵⁷ P. K. Behera,⁵⁸ L. Gladney,⁵⁸ Q. H. Guo,⁵⁸ J. Panetta,⁵⁸ M. Biasini,⁵⁹ R. Covarelli,⁵⁹ S. Pacetti,⁵⁹ M. Pioppi,⁵⁹ C. Angelini,⁶⁰ G. Batignani,⁶⁰ S. Bettarini,⁶⁰ F. Bucci,⁶⁰ G. Calderini,⁶⁰ M. Carpinelli,⁶⁰ R. Cenci,⁶⁰ F. Forti,⁶⁰ M. A. Giorgi,⁶⁰ A. Lusiani,⁶⁰ G. Marchiori,⁶⁰ M. Morganti,⁶⁰ N. Neri,⁶⁰ E. Paoloni,⁶⁰ M. Rama,⁶⁰ G. Rizzo,⁶⁰ J. Walsh,⁶⁰ M. Haire,⁶¹ D. Judd,⁶¹ D. E. Wagoner,⁶¹ J. Biesiada,⁶² N. Danielson,⁶² P. Elmer,⁶² Y. P. Lau,⁶² C. Lu,⁶² J. Olsen,⁶² A. J. S. Smith,⁶² A. V. Telnov,⁶² F. Bellini,⁶³ G. Cavoto,⁶³ A. D’Orazio,⁶³ E. Di Marco,⁶³ R. Faccini,⁶³ F. Ferrarotto,⁶³ F. Ferroni,⁶³ M. Gaspero,⁶³ L. Li Gioi,⁶³ M. A. Mazzoni,⁶³ S. Morganti,⁶³ G. Piredda,⁶³ F. Polci,⁶³ F. Safai Tehrani,⁶³ C. Voena,⁶³ H. Schröder,⁶⁴ R. Waldi,⁶⁴ T. Adye,⁶⁵ N. De Groot,⁶⁵ B. Franek,⁶⁵ G. P. Gopal,⁶⁵ E. O. Olaiya,⁶⁵ F. F. Wilson,⁶⁵ R. Aleksan,⁶⁶ S. Emery,⁶⁶ A. Gaidot,⁶⁶ S. F. Ganzhur,⁶⁶ G. Graziani,⁶⁶ G. Hamel de Monchenault,⁶⁶ W. Kozanecki,⁶⁶ M. Legendre,⁶⁶ G. W. London,⁶⁶ B. Mayer,⁶⁶ G. Vasseur,⁶⁶ Ch. Yèche,⁶⁶ M. Zito,⁶⁶ M. V. Purohit,⁶⁷ A. W. Weidemann,⁶⁷ J. R. Wilson,⁶⁷ T. Abe,⁶⁸ M. T. Allen,⁶⁸ D. Aston,⁶⁸ R. Bartoldus,⁶⁸ N. Berger,⁶⁸ A. M. Boyarski,⁶⁸ O. L. Buchmueller,⁶⁸ R. Claus,⁶⁸ J. P. Coleman,⁶⁸ M. R. Convery,⁶⁸ M. Cristinziani,⁶⁸ J. C. Dingfelder,⁶⁸ D. Dong,⁶⁸ J. Dorfan,⁶⁸ D. Dujmic,⁶⁸ W. Dunwoodie,⁶⁸ S. Fan,⁶⁸ R. C. Field,⁶⁸ T. Glanzman,⁶⁸ S. J. Gowdy,⁶⁸ T. Hadig,⁶⁸ V. Halyo,⁶⁸ C. Hast,⁶⁸ T. Hryn’ova,⁶⁸ W. R. Innes,⁶⁸ M. H. Kelsey,⁶⁸ P. Kim,⁶⁸ M. L. Kocian,⁶⁸ D. W. G. S. Leith,⁶⁸ J. Libby,⁶⁸ S. Luitz,⁶⁸ V. Luth,⁶⁸ H. L. Lynch,⁶⁸ H. Marsiske,⁶⁸ R. Messner,⁶⁸ D. R. Muller,⁶⁸ C. P. O’Grady,⁶⁸ V. E. Ozcan,⁶⁸ A. Perazzo,⁶⁸ M. Perl,⁶⁸ B. N. Ratcliff,⁶⁸ A. Roodman,⁶⁸ A. A. Salnikov,⁶⁸ R. H. Schindler,⁶⁸ J. Schwiening,⁶⁸ A. Snyder,⁶⁸ J. Stelzer,⁶⁸ D. Su,⁶⁸ M. K. Sullivan,⁶⁸ K. Suzuki,⁶⁸ S. K. Swain,⁶⁸ J. M. Thompson,⁶⁸ J. Va’vra,⁶⁸ N. van Bakel,⁶⁸ M. Weaver,⁶⁸ A. J. R. Weinstein,⁶⁸ W. J. Wisniewski,⁶⁸ M. Wittgen,⁶⁸ D. H. Wright,⁶⁸ A. K. Yarritu,⁶⁸ K. Yi,⁶⁸ C. C. Young,⁶⁸ P. R. Burchat,⁶⁹ A. J. Edwards,⁶⁹ S. A. Majewski,⁶⁹ B. A. Petersen,⁶⁹ C. Roat,⁶⁹ M. Ahmed,⁷⁰ S. Ahmed,⁷⁰ M. S. Alam,⁷⁰ R. Bula,⁷⁰ J. A. Ernst,⁷⁰ M. A. Saeed,⁷⁰ F. R. Wappler,⁷⁰ S. B. Zain,⁷⁰ W. Bugg,⁷¹ M. Krishnamurthy,⁷¹ S. M. Spanier,⁷¹ R. Eckmann,⁷² J. L. Ritchie,⁷² A. Satpathy,⁷² R. F. Schwitters,⁷² J. M. Izen,⁷³ I. Kitayama,⁷³ X. C. Lou,⁷³ S. Ye,⁷³ F. Bianchi,⁷⁴ M. Bona,⁷⁴ F. Gallo,⁷⁴ D. Gamba,⁷⁴ M. Bomben,⁷⁵ L. Bosisio,⁷⁵ C. Cartaro,⁷⁵ F. Cossutti,⁷⁵ G. Della Ricca,⁷⁵ S. Dittongo,⁷⁵ S. Grancagnolo,⁷⁵ L. Lancieri,⁷⁵ L. Vitale,⁷⁵ V. Azzolini,⁷⁶ F. Martinez-Vidal,⁷⁶ R. S. Panvini,^{77,‡} Sw. Banerjee,⁷⁸ B. Bhuyan,⁷⁸ C. M. Brown,⁷⁸ D. Fortin,⁷⁸ K. Hamano,⁷⁸ R. Kowalewski,⁷⁸ I. M. Nugent,⁷⁸ J. M. Roney,⁷⁸ R. J. Sobie,⁷⁸ J. J. Back,⁷⁹ P. F. Harrison,⁷⁹ T. E. Latham,⁷⁹ G. B. Mohanty,⁷⁹ H. R. Band,⁸⁰ X. Chen,⁸⁰ B. Cheng,⁸⁰ S. Dasu,⁸⁰ M. Datta,⁸⁰ A. M. Eichenbaum,⁸⁰ K. T. Flood,⁸⁰ M. T. Graham,⁸⁰ J. J. Hollar,⁸⁰ J. R. Johnson,⁸⁰ P. E. Kutter,⁸⁰ H. Li,⁸⁰ R. Liu,⁸⁰ B. Mellado,⁸⁰ A. Mihalyyi,⁸⁰ A. K. Mohapatra,⁸⁰ Y. Pan,⁸⁰ M. Pierini,⁸⁰ R. Prepost,⁸⁰ P. Tan,⁸⁰ S. L. Wu,⁸⁰ Z. Yu,⁸⁰ and H. Neal⁸¹

(The BABAR Collaboration)

¹Laboratoire de Physique des Particules, F-74941 Annecy-le-Vieux, France

²IFAE, Universitat Autònoma de Barcelona, E-08193 Bellaterra, Barcelona, Spain

³Università di Bari, Dipartimento di Fisica and INFN, I-70126 Bari, Italy

⁴Institute of High Energy Physics, Beijing 100039, China

⁵University of Bergen, Institute of Physics, N-5007 Bergen, Norway

⁶Lawrence Berkeley National Laboratory and University of California, Berkeley, California 94720, USA

⁷University of Birmingham, Birmingham, B15 2TT, United Kingdom

⁸Ruhr Universität Bochum, Institut für Experimentalphysik 1, D-44780 Bochum, Germany

⁹University of Bristol, Bristol BS8 1TL, United Kingdom

¹⁰University of British Columbia, Vancouver, British Columbia, Canada V6T 1Z1

¹¹Brunel University, Uxbridge, Middlesex UB8 3PH, United Kingdom

¹²Budker Institute of Nuclear Physics, Novosibirsk 630090, Russia

¹³University of California at Irvine, Irvine, California 92697, USA

- ¹⁴University of California at Los Angeles, Los Angeles, California 90024, USA
¹⁵University of California at Riverside, Riverside, California 92521, USA
¹⁶University of California at San Diego, La Jolla, California 92093, USA
¹⁷University of California at Santa Barbara, Santa Barbara, California 93106, USA
¹⁸University of California at Santa Cruz, Institute for Particle Physics, Santa Cruz, California 95064, USA
¹⁹California Institute of Technology, Pasadena, California 91125, USA
²⁰University of Cincinnati, Cincinnati, Ohio 45221, USA
²¹University of Colorado, Boulder, Colorado 80309, USA
²²Colorado State University, Fort Collins, Colorado 80523, USA
²³Universität Dortmund, Institut für Physik, D-44221 Dortmund, Germany
²⁴Technische Universität Dresden, Institut für Kern- und Teilchenphysik, D-01062 Dresden, Germany
²⁵Ecole Polytechnique, LLR, F-91128 Palaiseau, France
²⁶University of Edinburgh, Edinburgh EH9 3JZ, United Kingdom
²⁷Università di Ferrara, Dipartimento di Fisica and INFN, I-44100 Ferrara, Italy
²⁸Laboratori Nazionali di Frascati dell'INFN, I-00044 Frascati, Italy
²⁹Università di Genova, Dipartimento di Fisica and INFN, I-16146 Genova, Italy
³⁰Harvard University, Cambridge, Massachusetts 02138, USA
³¹Universität Heidelberg, Physikalisches Institut, Philosophenweg 12, D-69120 Heidelberg, Germany
³²Imperial College London, London, SW7 2AZ, United Kingdom
³³University of Iowa, Iowa City, Iowa 52242, USA
³⁴Iowa State University, Ames, Iowa 50011-3160, USA
³⁵Universität Karlsruhe, Institut für Experimentelle Kernphysik, D-76021 Karlsruhe, Germany
³⁶Laboratoire de l'Accélérateur Linéaire, F-91898 Orsay, France
³⁷Lawrence Livermore National Laboratory, Livermore, California 94550, USA
³⁸University of Liverpool, Liverpool L69 7ZE, United Kingdom
³⁹Queen Mary, University of London, E1 4NS, United Kingdom
⁴⁰University of London, Royal Holloway and Bedford New College, Egham, Surrey TW20 0EX, United Kingdom
⁴¹University of Louisville, Louisville, Kentucky 40292, USA
⁴²University of Manchester, Manchester M13 9PL, United Kingdom
⁴³University of Maryland, College Park, Maryland 20742, USA
⁴⁴University of Massachusetts, Amherst, Massachusetts 01003, USA
⁴⁵Massachusetts Institute of Technology, Laboratory for Nuclear Science, Cambridge, Massachusetts 02139, USA
⁴⁶McGill University, Montréal, Québec, Canada H3A 2T8
⁴⁷Università di Milano, Dipartimento di Fisica and INFN, I-20133 Milano, Italy
⁴⁸University of Mississippi, University, Mississippi 38677, USA
⁴⁹Université de Montréal, Physique des Particules, Montréal, Québec, Canada H3C 3J7
⁵⁰Mount Holyoke College, South Hadley, Massachusetts 01075, USA
⁵¹Università di Napoli Federico II, Dipartimento di Scienze Fisiche and INFN, I-80126, Napoli, Italy
⁵²NIKHEF, National Institute for Nuclear Physics and High Energy Physics, NL-1009 DB Amsterdam, The Netherlands
⁵³University of Notre Dame, Notre Dame, Indiana 46556, USA
⁵⁴Ohio State University, Columbus, Ohio 43210, USA
⁵⁵University of Oregon, Eugene, Oregon 97403, USA
⁵⁶Università di Padova, Dipartimento di Fisica and INFN, I-35131 Padova, Italy
⁵⁷Universités Paris VI et VII, Laboratoire de Physique Nucléaire et de Hautes Energies, F-75252 Paris, France
⁵⁸University of Pennsylvania, Philadelphia, Pennsylvania 19104, USA
⁵⁹Università di Perugia, Dipartimento di Fisica and INFN, I-06100 Perugia, Italy
⁶⁰Università di Pisa, Dipartimento di Fisica, Scuola Normale Superiore and INFN, I-56127 Pisa, Italy
⁶¹Prairie View A&M University, Prairie View, Texas 77446, USA
⁶²Princeton University, Princeton, New Jersey 08544, USA
⁶³Università di Roma La Sapienza, Dipartimento di Fisica and INFN, I-00185 Roma, Italy
⁶⁴Universität Rostock, D-18051 Rostock, Germany
⁶⁵Rutherford Appleton Laboratory, Chilton, Didcot, Oxon, OX11 0QX, United Kingdom
⁶⁶DSM/Dapnia, CEA/Saclay, F-91191 Gif-sur-Yvette, France
⁶⁷University of South Carolina, Columbia, South Carolina 29208, USA
⁶⁸Stanford Linear Accelerator Center, Stanford, California 94309, USA
⁶⁹Stanford University, Stanford, California 94305-4060, USA
⁷⁰State University of New York, Albany, New York 12222, USA
⁷¹University of Tennessee, Knoxville, Tennessee 37996, USA
⁷²University of Texas at Austin, Austin, Texas 78712, USA
⁷³University of Texas at Dallas, Richardson, Texas 75083, USA
⁷⁴Università di Torino, Dipartimento di Fisica Sperimentale and INFN, I-10125 Torino, Italy
⁷⁵Università di Trieste, Dipartimento di Fisica and INFN, I-34127 Trieste, Italy
⁷⁶IFIC, Universitat de Valencia-CSIC, E-46071 Valencia, Spain
⁷⁷Vanderbilt University, Nashville, Tennessee 37235, USA

⁷⁸University of Victoria, Victoria, British Columbia, Canada V8W 3P6
⁷⁹Department of Physics, University of Warwick, Coventry CV4 7AL, United Kingdom
⁸⁰University of Wisconsin, Madison, Wisconsin 53706, USA
⁸¹Yale University, New Haven, Connecticut 06511, USA

We report on searches for $B^- \rightarrow D_s^- \phi$ and $B^- \rightarrow D_s^{*-} \phi$. In the context of the Standard Model, these decays are expected to be highly suppressed since they proceed through annihilation of the b and \bar{u} quarks in the B^- meson. Our results are based on 234 million $\Upsilon(4S) \rightarrow B\bar{B}$ decays collected with the BABAR detector at SLAC. We find no evidence for these decays, and we set Bayesian 90% confidence level upper limits on the branching fractions $\mathcal{B}(B^- \rightarrow D_s^- \phi) < 1.9 \times 10^{-6}$ and $\mathcal{B}(B^- \rightarrow D_s^{*-} \phi) < 1.2 \times 10^{-5}$. These results are consistent with Standard Model expectations.

PACS numbers: 13.25.Hw, 12.60.Jv, 11.30.Pb

In the Standard Model (SM), the decay $B^- \rightarrow D_s^{(*)-} \phi$ occurs through annihilation of the two quarks in the B meson into a virtual W as shown in Figure 1. No pure W -annihilation B decays have ever been observed. The current upper limits on the branching fractions of $B^- \rightarrow D_s^- \phi$ and $B^- \rightarrow D_s^{*-} \phi$ are 3.2×10^{-4} (90% C.L.) and 4×10^{-4} (90% C.L.), respectively, set by the CLEO collaboration in 1993 [1].

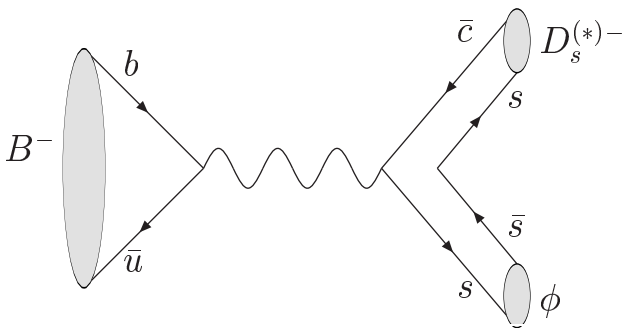


FIG. 1: Feynman diagram for $B^- \rightarrow D_s^{(*)-} \phi$.

In the SM, B annihilation amplitudes are highly suppressed. Calculations of the $B^- \rightarrow D_s^- \phi$ branching fraction give predictions of 3×10^{-7} using a perturbative QCD approach [2], 1.9×10^{-6} using factorization [3], and 7×10^{-7} using QCD-improved factorization [3].

Since the current experimental limits are about three orders of magnitude higher than the SM expectations, searches for $B^- \rightarrow D_s^{(*)-} \phi$ could be sensitive to new physics contributions. Reference [3] argues that the branching fraction for $B^- \rightarrow D_s^- \phi$ could be as high as 8×10^{-6} in a two-Higgs doublet model and 3×10^{-4} in the minimal supersymmetric model with R -parity violation, depending on the details of the new physics parameters.

Our results are based on $234 \times 10^6 \Upsilon(4S) \rightarrow B\bar{B}$ decays, corresponding to an integrated luminosity of 212 fb^{-1} , collected between 1999 and 2004 with the BABAR detector [4] at the PEP-II B Factory [5] at the Stanford Linear Accelerator Center. A 12 fb^{-1} off-resonance data sample, with a center-of-mass (CM) energy 40 MeV below the $\Upsilon(4S)$ resonance peak, is used to study contin-

uum events, $e^+e^- \rightarrow q\bar{q}$ ($q = u, d, s$, or c). The number of B mesons in our data sample is two orders of magnitudes larger than in the previously-published search [1].

We search for the decay $B^- \rightarrow D_s^{(*)-} \phi$ in the following modes: $D_s^{*-} \rightarrow D_s^- \gamma$, $D_s^- \rightarrow \phi \pi^-$, $K_s^0 K^-$, and $K^{*0} K^-$, with the secondary decay modes $\phi \rightarrow K^+ K^-$, $K_s^0 \rightarrow \pi^+ \pi^-$, and $K^{*0} \rightarrow K^+ \pi^-$. (Charge-conjugate decay modes are implied throughout this article.) We denote the ϕ from $B^- \rightarrow D_s^{(*)-} \phi$ as the “bachelor ϕ ” in order to distinguish it from the ϕ in $D_s^- \rightarrow \phi \pi^-$.

Our analysis strategy is the following. Starting from the set of reconstructed tracks and electromagnetic calorimeter clusters, we select events which are kinematically consistent with the $\Upsilon(4S) \rightarrow B\bar{B}$, $B^- \rightarrow D_s^{(*)-} \phi$ hypothesis. Backgrounds, mostly from continuum events, are suppressed using a likelihood constructed from a number of kinematical and event shape variables. For each candidate satisfying all selection criteria, we calculate the energy-substituted mass, m_{ES} , defined later in this article. The m_{ES} distribution of these events is then fit to a signal plus background hypothesis to extract the final signal yield.

All kaon candidate tracks in the reconstructed decay chains must satisfy a set of loose kaon identification criteria based on the response of the internally-reflecting ring-imaging Cherenkov radiation detector and the ionization measurements in the drift chamber and the silicon vertex tracker. The kaon selection efficiency is a function of momentum and polar angle, and is typically 95%. These requirements provide a rejection factor of order 10 against pion backgrounds. No particle identification requirements are imposed on pion candidate tracks.

We select ϕ , K_s^0 , and K^{*0} candidates from pairs of oppositely-charged tracks with invariant masses consistent with the parent particle decay hypothesis and consistent with originating from a common vertex. The invariant mass requirements are $\pm 10 \text{ MeV}$ ($\sim 2.4\Gamma$) for the ϕ , $\pm 9 \text{ MeV}$ ($\sim 3\sigma$) for the K_s^0 , and $\pm 75 \text{ MeV}$ ($\sim 1.5\Gamma$) for the K^{*0} , where σ and Γ are the experimental and natural width, respectively, of these particles. (Here, and throughout the paper, we use natural units where $c = 1$.) We then form D_s^- candidates in the three modes listed above by combining ϕ , K_s^0 , or K^{*0} candidates with an

additional track. The invariant mass of the D_s^- candidate must be within 15 MeV ($\sim 3\sigma$) of the known D_s^- mass. In the $D_s^- \rightarrow \phi\pi^-$ and $D_s^- \rightarrow K^{*0}K^-$ modes, all three charged tracks are required to originate from a common vertex. In the $D_s^- \rightarrow K_s^0K^-$ mode, the K_s^0 and D_s^- vertices are required to be separated by at least 3 mm. This last requirement is very effective in rejecting combinatorial background and is 94% efficient for signal. We select D_s^{*-} candidates from D_s^- and photon candidates. The photon candidates are constructed from calorimeter clusters with lateral profiles consistent with photon showers and with energy above 60 MeV in the laboratory frame. We require that the mass difference $\Delta M \equiv M(D_s^{*-}) - M(D_s^-)$ be between 130 and 156 MeV. The ΔM resolution is about 5 MeV.

At each stage in the reconstruction, the measurement of the momentum vector of an intermediate particle is improved by refitting the momenta of the decay products with kinematical constraints. These constraints are based on the known mass [6] of the intermediate particle and on the fact that the decay products must originate from a common point in space.

Finally, we select B^- candidates by combining $D_s^{(*)-}$ and bachelor ϕ candidates. A B^- candidate is characterized kinematically by the energy-substituted mass $m_{\text{ES}} \equiv \sqrt{(\frac{1}{2}s + \vec{p}_0 \cdot \vec{p}_B)^2 / E_0^2 - \vec{p}_B^2}$ and energy difference $\Delta E \equiv E_B^* - \frac{1}{2}\sqrt{s}$, where E and \vec{p} are energy and momentum, the asterisk denotes the CM frame, the subscripts 0 and B refer to the initial $\Upsilon(4S)$ and B candidate, respectively, and s is the square of the CM energy. In the CM frame, m_{ES} reduces to $m_{\text{ES}} = \sqrt{\frac{1}{4}s - \vec{p}_B^{*2}}$. For signal events we expect $m_{\text{ES}} \sim M_B$, the known B^- mass, and $\Delta E \sim 0$. The resolutions of m_{ES} and ΔE are approximately 2.6 MeV and 10 MeV, respectively. For events with more than one B^- candidate, we retain the candidate with the lowest χ^2 computed from the measured values, known values, and resolutions for the D_s^- mass, the bachelor ϕ mass, and, where applicable, ΔM .

This analysis was performed blind: GEANT4 simulated data [7] or data samples outside the fit region were used for background studies and selection criteria optimization. Most of the backgrounds to the $B^- \rightarrow D_s^{(*)-}\phi$ signal were determined to be from continuum events. To reduce these backgrounds we make two additional requirements. First, we require $|\cos\theta_T| < 0.9$, where θ_T is the angle between the thrust axis of the B^- candidate and the rest of the tracks and neutral clusters in the event, calculated in the CM frame. The distribution of $|\cos\theta_T|$ is essentially uniform for signal events and strongly peaked near unity for continuum events. Second, for each event we define a relative likelihood for signal and background based on a number of kinematical quantities. The relative likelihood is defined as the ratio of the likelihoods for signal and background. The sig-

nal (background) likelihood is defined as the product of the probability density functions, PDFs, for the various kinematical quantities in signal (background) events.

The kinematical quantities used in the likelihood are reconstructed masses, helicity angles, and a Fisher discriminant designed to distinguish between continuum and $B\bar{B}$ events; we will discuss each of these in turn in the following paragraphs. All PDFs are chosen based on studies of Monte Carlo and off-resonance data.

The masses used in the likelihoods are those of the D_s^- , ΔM for $D_s^{*-} \rightarrow D_s\gamma$, the K^{*0} in $D_s^- \rightarrow K^{*0}K^-$, and the ϕ in $D_s^- \rightarrow \phi\pi^-$. The signal PDFs for the mass variables are the sum of two Gaussian distributions for D_s^- and ΔM , a Breit-Wigner distribution for the K^{*0} , and a Voigtian distribution [8] for the ϕ . We parameterize the background PDFs as uniform distributions. Note that the mass of the bachelor ϕ and the mass of the K_s^0 in $D_s^- \rightarrow K_s^0K^-$ are not used in the definition of the likelihoods. This is because studies of background event samples suggest that background events contain mostly real bachelor ϕ and real K_s^0 mesons.

The helicity angles used in the likelihood are those in $K^{*0} \rightarrow K^+\pi^-$ and in $\phi \rightarrow K^+K^-$ for both ϕ candidates. The signal PDFs for these quantities are set by angular momentum conservation to be proportional to $\cos^2\theta$, where θ is the helicity angle for the process. The one exception is the helicity angle distribution of the bachelor ϕ in $B^- \rightarrow D_s^{*-}\phi$, where the polarization of the two vector mesons in the final state is not known. For this reason, the helicity angle of the bachelor ϕ is not used in the definition of the likelihood for the $B^- \rightarrow D_s^{*-}\phi$ mode. The background PDFs for these variables are uniform in $\cos\theta$. In addition, in the likelihood we also use the polar angle of the B^- candidate in the CM frame (θ_B). The signal is expected to follow a $\sin^2\theta_B$ distribution, while the background is independent of $\cos\theta_B$.

The final component of the likelihood is a Fisher discriminant constructed from the quantities $L_0 = \sum_i p_i^*$ and $L_2 = \sum_i p_i^* \cos^2\alpha_i^*$. Here, p_i^* is the magnitude of the momentum and α_i^* is the angle with respect to the thrust axis of the B^- candidate of tracks and clusters not used to reconstruct the B^- , all in the CM frame. The signal and background PDFs for this variable are modeled as bifurcated Gaussians with different means and standard deviations. Note that the likelihood is constructed to have negligible correlations between its components. Since the Fisher discriminant is highly correlated with the $|\cos\theta_T|$ variable defined above, the $|\cos\theta_T|$ variable is treated separately and not included in the likelihood.

The likelihood requirements have been optimized to maximize the expected sensitivity on a mode-by-mode basis. (The expected sensitivity is defined as the branching ratio upper limit that we should obtain, on average, when performing this experiment many times in the absence of a signal.) Depending on the mode, the combined efficiency of the likelihood and the $|\cos\theta_T|$ requirements

TABLE I: Efficiencies (ϵ), branching fractions (\mathcal{B}), and products of efficiency and branching fractions for the modes used in the $B^- \rightarrow D_s^{(*)-} \phi$ search. The uncertainties on the ϵ and \mathcal{B} are discussed in the text. Here \mathcal{B} is the product of branching fractions for the secondary and tertiary decays in the specified decay mode.

B Mode	D_s^- Mode	ϵ	$\mathcal{B}(10^{-3})$	$\epsilon \times \mathcal{B}(10^{-3})$
$B^- \rightarrow D_s^- \phi$				
	$D_s^- \rightarrow \phi \pi^-$	0.192	11.6	2.22
	$D_s^- \rightarrow K^- K_s^0$	0.177	8.2	1.45
	$D_s^- \rightarrow K^{*0} K^-$	0.140	14.5	2.03
$B^- \rightarrow D_s^{*-} \phi$				
	$D_s^- \rightarrow \phi \pi^-$	0.109	10.9	1.19
	$D_s^- \rightarrow K^- K_s^0$	0.100	7.7	0.77
	$D_s^- \rightarrow K^{*0} K^-$	0.083	13.6	1.14

varies between 71% and 83%, while providing a rejection factor of between 4 and 7 against continuum backgrounds.

After applying the requirements on relative likelihood and $|\cos \theta_T|$, we also demand that ΔE fall inside the signal region: within 30 MeV ($\sim 3\sigma$) of its expected mean value for signal events. This mean value is determined from simulation, and varies between -3 and 0 MeV, depending on the mode.

The efficiencies of our selection requirements, shown in Table I, are determined from simulations. For the $B^- \rightarrow D_s^{*-} \phi$ mode, we take the average of the efficiencies calculated assuming fully longitudinal or transverse polarization for the two vector meson final state. These efficiencies are found to be the same to within 1%. The quantities \mathcal{B} in Table I are the product of the known branching fractions for the secondary and tertiary decay modes. These are taken from the compilation of the Particle Data Group [6], with the exception of the branching fraction for $D_s^- \rightarrow \phi \pi^-$, for which we use the latest, most precise measurement $\mathcal{B}(D_s^- \rightarrow \phi \pi^-) = (4.8 \pm 0.6)\%$ [9]. Since the branching fractions for the other two D_s^- modes are measured with respect to the $D_s^- \rightarrow \phi \pi^-$ mode, we have rescaled their tabulated values from the Particle Data Group accordingly.

The systematic uncertainties on the products of efficiency and branching ratio for the secondary decays in the decay chain of interest are summarized in Table II. The largest systematic uncertainty is associated with the uncertainty on the $D_s^- \rightarrow \phi \pi^-$ branching ratio, which is only known to 13% [9], and which is used to normalize all other D_s^- branching ratios.

The experimental systematic uncertainties all relate to the determination of the efficiency, ϵ . The dominant source of error is the uncertainty in the efficiency of the kaon identification requirements. The efficiency of these requirements is calibrated using a sample of kinematically identified $D^{*0} \rightarrow D^0 \pi^+$, $D^0 \rightarrow K^- \pi^+$ de-

TABLE II: Systematic uncertainties on $\sum_i \epsilon_i \cdot \mathcal{B}_i$, where the index i runs over the three D_s^- modes used in this analysis, ϵ_i are the experimental efficiencies, and \mathcal{B}_i are the branching fractions for the i^{th} mode.

Source	$B^- \rightarrow D_s^- \phi$	$B^- \rightarrow D_s^{*-} \phi$
D_s^- branching fraction	14%	14%
D_s^{*-} branching fraction	—	2.5%
Other branching fractions	1.5%	1.5%
Charged kaon ID	13.2%	13.3%
Tracking and K_s^0 efficiency	3.7%	3.7%
Photon efficiency	—	1.8%
Final state polarization	—	1%
Selection requirements	5%	5%
Simulation statistics	0.6%	0.6%
Total	20%	21%

cays, where track quality selection differences between this sample and our analysis sample have been taken into account. The efficiency of the kaon identification requirements is assigned a 3.6% systematic error. This results in a systematic uncertainty of 14% for the efficiency of the modes with four charged kaons ($D_s^- \rightarrow K^{*0} K^-$, $D_s^- \rightarrow \phi \pi^-$), and 11% for the mode with three charged kaons ($D_s^- \rightarrow K_s^0 K^-$). A second class of uncertainties is associated with the detection efficiency for tracks and clusters. From studies of a variety of control samples, the tracking efficiency is understood at the level of 1.4% (0.6%) for transverse momenta below (above) 200 MeV. There is also a 1.9% uncertainty associated with the reconstruction of $K_s^0 \rightarrow \pi^+ \pi^-$ which can occur a few centimeters away from the interaction point. Given the multiplicity and momentum spectrum of tracks in the decay modes of interest, the uncertainty on the efficiency of reconstructing tracks in the B -decay chain is estimated to be 3.7%. In the $B^- \rightarrow D_s^{*-} \phi$ search, there is an additional uncertainty of 1.8% due to the uncertainty on the efficiency to reconstruct the photon in $D_s^{*-} \rightarrow D_s \gamma$, and a 1% uncertainty from the unknown polarization in the final state. Finally, to ascertain the systematic uncertainty due to the efficiency of the other event selection requirements, we examine the variation of the efficiency under differing conditions: shifting the ΔE by 3 MeV (0.3%); shifting the mean of the D_s^- and ϕ masses and ΔM by 1 MeV (0.2%, 0.1%, 0.2%, respectively); increasing the width of the D_s^- and ϕ masses and ΔM by 1 MeV (1.5%, 0.4%, 1.5%, respectively); using a Fisher distribution obtained from the data sample of a similar analysis, $B \rightarrow D \pi$ with $D \rightarrow K \pi$ (3%). Thus we assign a 5% systematic on the combined efficiency of these selection criteria.

We determine the yield of signal events from an unbinned extended maximum-likelihood fit to the m_{ES} distribution of B^- candidates satisfying all of the requirements listed above. We fit simultaneously in two

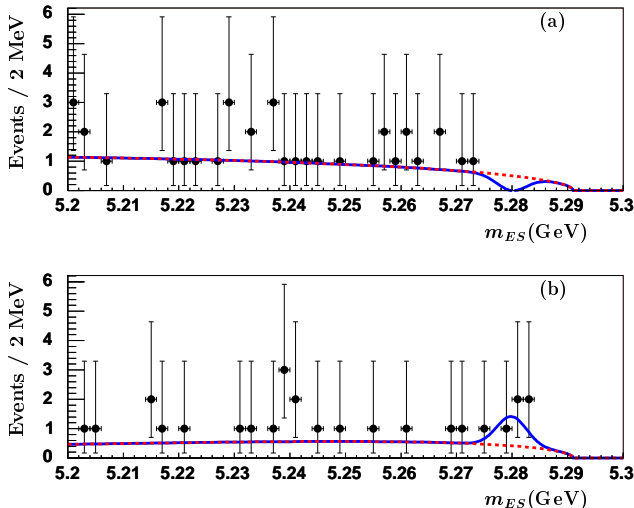


FIG. 2: Distribution of m_{ES} for (a) $B^- \rightarrow D_s^- \phi$ and (b) $B^- \rightarrow D_s^{*-} \phi$ candidates in the $|\Delta E|$ signal region. The superimposed curves are the result of the fits described in the text. The dashed curve is the background contribution and the solid curve is the sum of the signal and background components.

$|\Delta E|$ regions: in the signal region the distribution is parametrized as a Gaussian and the combinatorial background as a threshold function [11]; in a sideband of ΔE ($|\Delta E| < 200$ MeV, excluding the signal region) we fit solely for the threshold function parameter. In our fit, the amplitude of the Gaussian is allowed to fluctuate to negative values, but, for reasons of numerical stability, the sum of the Gaussian and the threshold function is constrained to be positive over the full m_{ES} fit range. The mean and the standard deviations of the Gaussian are constrained to the values determined from Monte Carlo simulation. The fitting procedure was extensively tested with sets of simulated data, and was found to provide an unbiased estimate of the signal yield.

Figure 2 shows the m_{ES} distribution of the selected candidates. We see no evidence for $B^- \rightarrow D_s^{(*)-} \phi$. The fitted event yields are $N = -1.6_{-0.0}^{+0.7}$ and $N = 3.4_{-2.1}^{+2.8}$ for the $B^- \rightarrow D_s^- \phi$ and $B^- \rightarrow D_s^{*-} \phi$ modes, respectively, where the quoted uncertainties correspond to changes of 0.5 in the log-likelihood for the fit. The likelihood curves are shown in Figure 3. The requirement that the sum of the Gaussian and the threshold function be always positive results in an effective constraint $N > -1.6$ in the $B^- \rightarrow D_s^- \phi$ mode. This is the source of the sharp edge at $N = -1.6$ in the likelihood distribution of Figure 3(a).

We use a Bayesian approach with a flat prior to set 90% confidence level upper limits on the branching fractions for the $B^- \rightarrow D_s^- \phi$ and $B^- \rightarrow D_s^{*-} \phi$ modes. In a given mode, the upper limit on the number of observed events

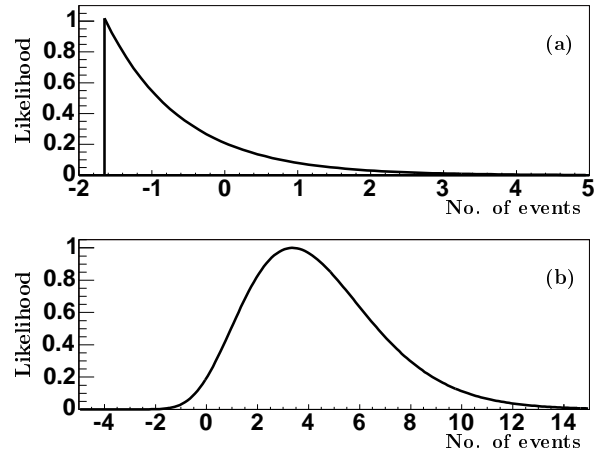


FIG. 3: Likelihood from the fit in arbitrary units as a function of the number of signal events. (a) $B^- \rightarrow D_s^- \phi$; (b) $B^- \rightarrow D_s^{*-} \phi$.

(N_{UL}) is defined as

$$\int_0^{N_{UL}} \mathcal{L}(N) dN = 0.9 \int_0^{+\infty} \mathcal{L}(N) dN. \quad (1)$$

$\mathcal{L}(N)$ is the likelihood, determined from the m_{ES} fit detailed above, as a function of the number of signal events, N . The upper limit \mathcal{B} on the branching fraction is

$$\mathcal{B} < \frac{N_{UL}}{N_{B\bar{B}} \sum_i \epsilon_i \times \mathcal{B}_i}. \quad (2)$$

$N_{B\bar{B}} = (233.9 \pm 2.5) \times 10^6$ is the number of $B\bar{B}$ events, the index i runs over the three D_s^- decay modes, ϵ_i is the efficiency in the i^{th} mode, and \mathcal{B}_i is the product of all secondary and tertiary branching fractions (see Table I).

We account for systematic uncertainties by numerically convolving $\mathcal{L}(N)$ with a Gaussian distribution with its width determined by the total systematic uncertainties (Table II) in the two modes, including the 1.1% uncertainty in $N_{B\bar{B}}$ added in quadrature. We find limits $\mathcal{B}(B^- \rightarrow D_s^- \phi) < 1.9 \times 10^{-6}$ and $\mathcal{B}(B^- \rightarrow D_s^{*-} \phi) < 1.2 \times 10^{-5}$ at the 90% confidence level. These limits are calculated using $\mathcal{B}(D_s^- \rightarrow \phi\pi^-) = (4.8 \pm 0.6)\%$ from Reference [9]. If we were to use the value $\mathcal{B}(D_s^- \rightarrow \phi\pi^-) = (3.6 \pm 0.9)\%$ from the Particle Data Group [6], we would find $\mathcal{B}(B^- \rightarrow D_s^- \phi) < 2.7 \times 10^{-6}$ and $\mathcal{B}(B^- \rightarrow D_s^{*-} \phi) < 1.7 \times 10^{-5}$. For completeness, we also compute $\mathcal{B}(B^- \rightarrow D_s^- \phi) \times \mathcal{B}(D_s^- \rightarrow \phi\pi^-) < 8.6 \times 10^{-8}$ and $\mathcal{B}(B^- \rightarrow D_s^{*-} \phi) \times \mathcal{B}(D_s^- \rightarrow \phi\pi^-) < 5.4 \times 10^{-7}$, also at the 90% confidence level.

In summary, we have searched for $B^- \rightarrow D_s^{(*)-} \phi$, and we have found no evidence for these decays. Our limits are about two orders of magnitude lower than the previous results, but are still one order of magnitude higher than the Standard Model expectation.

Using the calculation of Reference [3], we can use our results to set bounds on new physics contributions. These bounds are obtained in the framework of factorization, neglecting systematic uncertainties associated with the calculation of hadronic effects. In the type II Two-Higgs-Doublet model we extract a tree-level 90% C.L. limit $\tan\beta/M_H < 0.37/\text{GeV}$, where $\tan\beta$ is the ratio of the vacuum expectation values for the two Higgs doublets and M_H is the mass of the charged Higgs boson. This limit is not quite as stringent as the limit that can be obtained from the $B^- \rightarrow \tau^- \nu_\tau$ decay mode, $\tan\beta/M_H < 0.29/\text{GeV}$ [12].

In the context of supersymmetric models with R -parity violation (RPV) [3, 13], the new physics contribution to $B \rightarrow D_s \phi$ depends on the quantity $\frac{\lambda^2}{M^2} \equiv \sum_i \frac{\lambda'_{2i2} \lambda'_{i13}}{M_i^2}$, where λ'_{jkl} is the coupling between the j^{th} generation doublet lepton superfield, the k^{th} generation doublet quark superfield, and the l^{th} generation singlet down-type quark superfield; M_i is the mass of the i^{th} generation charged super-lepton. Conservatively assuming maximal destructive interference between the SM and RPV amplitudes, we find $|\frac{\lambda^2}{M^2}| < 4 \times 10^{-4}/(100 \text{ GeV})^2$.

We are grateful for the excellent luminosity and machine conditions provided by our PEP-II colleagues, and for the substantial dedicated effort from the computing organizations that support *BABAR*. The collaborating institutions wish to thank SLAC for its support and kind hospitality. This work is supported by DOE and NSF (USA), NSERC (Canada), IHEP (China), CEA and CNRS-IN2P3 (France), BMBF and DFG (Germany), INFN (Italy), FOM (The Netherlands), NFR (Norway), MIST (Russia), and PPARC (United Kingdom). Indi-

viduals have received support from CONACyT (Mexico), A. P. Sloan Foundation, Research Corporation, and Alexander von Humboldt Foundation.

* Also with Università di Perugia, Dipartimento di Fisica, Perugia, Italy

† Also with Università della Basilicata, Potenza, Italy

‡ Deceased

- [1] CLEO Collaboration, J. P. Alexander *et al.*, *Phys. Lett.* **B319**, 365 (1993).
- [2] C. D. Lu, *Eur. Phys. J.* **C24**, 121 (2002).
- [3] R. Mohanta, *Phys. Lett.* **B540**, 241 (2002).
- [4] *BABAR* Collaboration, B. Aubert *et al.*, *Nucl. Instr. and Methods* **A479**, 1 (2002).
- [5] PEP-II Conceptual Design Report, SLAC-0418 (1993).
- [6] S. Eidelman *et al.*, *Phys. Lett.* **B592**, 1 (2004).
- [7] S. Agostinelli *et al.* *Nucl. Instr. and Methods A* **506**, 250 (2003).
- [8] A Voigtian is the convolution of a Breit-Wigner lineshape with a Gaussian resolution term.
- [9] *BABAR* Collaboration, B. Aubert *et al.*, *Phys. Rev.* **D71**, 091104(R) (2005).
- [10] *BABAR* Collaboration, B. Aubert *et al.*, *Phys. Rev.* **D70**, 011101 (2004).
- [11] The function is $f(m_{ES}) \propto m_{ES} \sqrt{1-x^2} \exp[-\zeta(1-x^2)]$, where $x = 2m_{ES}/\sqrt{s}$ and ζ is a fit parameter; ARGUS Collaboration, H. Albrecht *et al.*, *Z. Phys.* **C48**, 543 (1990).
- [12] Belle Collaboration, K. Abe *et al.*, hep-ex/0507034.
- [13] See, for example, H. Dreiner, *An Introduction to Explicit R-Parity Violation in Perspectives on Supersymmetry*, p.462-479, Ed. G.L. Kane (World Scientific).